Hydrogen dynamics in heavy alkali metal hydrides obtained through inelastic neutron scattering

2004 J. Phys.: Condens. Matter 16 5731

(http://iopscience.iop.org/0953-8984/16/32/010)

INSTITUTE OF PHYSICS PUBLISHING JOURNAL OF PHYSICS: CONDENSED MATTER

J. Phys.: Condens. Matter **16** (2004) 5731–5743 PII: S0953-8984(04)77739-5

Hydrogen dynamics in heavy alkali metal hydrides obtained through inelastic neutron scattering

G Auffermann[1], G D Barrera[2], D Colognesi[3], G Corradi[3], A J Ramirez-Cuesta[4] and M Zoppi[3]

[1] Max-Planck-Institut für Chemische Physik fester Stoffe, Nöthnitzer Straße 40, 01187 Dresden, Germany
[2] Departamento de Química, Universidad Nacional de la Patagonia SJB, Ciudad Universitaria, 9005 Comodoro Rivadavia, Argentina
[3] Consiglio Nazionale delle Ricerche, Istituto di Fisica Applicata 'Nello Carrara', via Madonna del Piano, 50019 Sesto Fiorentino (FI), Italy
[4] ISIS facility, Rutherford Appleton Laboratory, Chilton, Didcot, OX11 0QX, UK

Received 12 March 2004
Published 30 July 2004
Online at stacks.iop.org/JPhysCM/16/5731
doi:10.1088/0953-8984/16/32/010

Abstract

Inelastic neutron scattering spectra from polycrystalline NaH, KH, RbH and CsH, measured at low temperature in the energy transfer range 3 meV $< E <$ 500 meV, are reported. From the medium-energy regions, coinciding with the optical phonon bands, accurate hydrogen-projected densities of phonon states are extracted and compared to *ab initio* lattice dynamics results. The overall agreement is very good. Further lattice dynamics calculations, based on a pairwise Born–Mayer semi-empirical potential scheme, were also performed, providing only limited and qualitative agreement with the experimental data. In conclusion, incoherent inelastic neutron spectroscopy proves to be a stringent validation tool for lattice dynamics simulations of H-containing materials.

1. Introduction

Hydrogen forms stable hydrides by reaction with all alkali metals: Li, Na, K, Rb, Cs [1]. The first x-ray diffraction studies in 1931 [2] showed that LiH, NaH, KH, RbH and CsH (AlkH for short) crystallize with the rock-salt structure at ambient pressure. In these materials, evidence seems to be consistent with hydrogen being present in the form of anions or modified anions: electron distribution investigations [3] estimated the H ionic effective charge in AlkH to fall in the range from -0.93 to -1.11 electron charges, indicating that alkali metal hydrides are probably very similar to alkali metal halides, as regards the electronic structure, so AlkH might be even regarded as the 'lightest alkali metal halides', not far from alkali metal fluorides. In view of this feature, which gives rise to long-range interactions between hydrogen atoms, the H dynamics in these compounds is expected to be very different from that in group 3–7

metal hydrides. However, virtually only LiH (and LiD) have been extensively studied [4], both theoretically and experimentally, while much work has been carried out on the various alkali fluorides. The choice of lithium hydride (and deuteride) has not been casual: they are rock-salt quantum crystals having only four electrons per asymmetric unit, which makes them the simplest ionic crystals in terms of electronic structure. Moreover, there is a large isotopic effect provided by proton and deuteron exchange. Because of these unique physical properties and because of their use in thermonuclear weapons, LiH and LiD lattices are well described, both structurally (neutron diffraction) [5] and dynamically (second-order Raman spectroscopy [6] and inelastic neutron scattering [7–9]). However, as far as NaH, KH, RbH and CsH are concerned, besides incomplete experimental studies on NaH vibrational spectra [9], only lattice dynamics calculation has been reported so far, in [10]. In that paper, extended versions of the deformation dipole model and the shell model were investigated for the lattice dynamics of LiH and LiD. The best fit to the phonon dispersion curve of LiD was obtained with a deformation dipole model with 13 adjustable parameters (DDM13), which also provided elastic and dielectric constants, effective charges, second-order Raman spectra and densities of phonon states (DoPS). In addition, the phonon dispersion curves of the deuterides of Na, K, Rb and Cs were also presented. They were based on a simple shell model (SM), whose parameters have been deduced from the force constants and the ionic charge of LiD as well as the polarizabilities of the ions, since no experimental information on the dynamics of these crystals was available at that time. Given the aforementioned scenario, a detailed experimental study on the whole series of alkali metal hydrides is highly desirable in order to provide the first spectroscopic measurements on NaH, KH, RbH and CsH. Actually only the reststrahlung frequency for CsH is known [11]. As a matter of fact, some intriguing questions arise in connection with hydrogen vibrational dynamics in AlkH: How is the H motion described by the proposed force constant model [10]? And by the various potential schemes [12]? How do they compare with the present incoherent inelastic neutron scattering data? We believe that a combined use of incoherent inelastic neutron scattering (IINS), from which the H-DoPS can be worked out, and of *ab initio* simulations, from which important physical quantities can be derived (lattice constants, bulk modulus, phonon dispersion curves and density of states etc) can provide a new and deep insight into the problem of the hydrogen dynamics in condensed matter. In this respect, the growing interest in lightweight hydrides as H-storage media makes this topic relevant for possible practical applications. In practice, AlkH can be considered as model compounds for more complex hydrogen compounds (MgH_2, aluminohydrides, borohydrides etc). Thus a validation of the *ab initio* calculations via the IINS spectra could represent an important step towards a complete description of the microscopic H dynamics in technologically relevant hydrides. In the present paper we study the vibrational motion of hydrogen in the series NaH to CsH by means of the inelastic neutron scattering technique. Section 2 will be devoted to the description of the experimental apparatus and the neutron scattering measurements. In section 3 we will show how to extract a reliable H-DoPS from the experimental spectra, while in section 4 the two simulation techniques used in this work will be briefly reviewed. Then in section 5 the results on the H dynamics in the heavy AlkH will be discussed and a comparison with the lattice dynamics simulations will be established. Finally, in section 6 we will present some conclusions and perspectives on this subject.

2. Experiment description

The IINS measurements were carried out using the TOSCA-II inelastic spectrometer of the ISIS pulsed neutron source at Rutherford Appleton Laboratory, Chilton, Didcot (UK). TOSCA-II

Table 1. Sample description, including experimental temperature, T, integrated proton current, IPC, mass, scattering power at incoming neutron energy of 70 meV, p, and purity.

Sample	T (K)	IPC (μA h)	Mass (g)	p (%)	Purity (wt%)
NaH	20.1(1)	660.5	3.1	13.21	95
KH	20.0(1)	3284.0	2.6	6.02	>97[a]
RbH	20.0(1)	3213.9	5.9	7.53	>97[a]
CsH	20.0(1)	3124.9	9.2	3.32	>95[a]

[a] No impurities were detected by x-ray powder diffraction experiments.

is a crystal-analyser inverse-geometry spectrometer [13], where the final neutron energy is selected through two sets of pyrolytic graphite crystal analysers placed in forward-scattering (at around 42.6° with respect to the incident beam) and in back-scattering (at about 137.7°). This arrangement fixes the nominal scattered neutron energy to $E_1 = 3.35$ meV (forward-scattering) and to $E_1 = 3.32$ meV (back-scattering). Higher-order Bragg reflections are filtered out by 120 mm thick beryllium blocks cooled down to a temperature lower than 30 K. The incident neutron beam, on the other hand, spans a broad energy range allowing coverage of an extended energy transfer ($E = E_0 - E_1$) region: 3 meV $< E <$ 500 meV. Because of the fixed geometry of this spectrometer, the wavevector transfer, Q, is related to the energy transfer through a monotonic function, roughly proportional to the square root of the energy transfer: $Q = Q(E) \propto \sqrt{E}$. TOSCA-II has an excellent energy resolution in the accessible energy transfer range ($\Delta E/E_0 \cong$ 1.5–3%). The sample cell used for NaH was made of aluminium with a slab geometry (47 × 34 mm^2, 5 mm thick). Special care was devoted to preventing possible sodium hydroxide formation during the sample loading procedure. The measurements on KH, RbH and CsH required, in contrast, a different choice of the sample container, due to the very unstable and sensitive nature of these hydrides [1]. After their syntheses they were accurately sealed in square quartz cells (40 × 40 mm^2, 7.5 mm thick). In table 1 we have summarized various experimental details concerning the five alkali metal hydrides, all in the form of polycrystalline powder as checked by means of standard x-ray diffraction. Before the AlkH measurements, the two empty cells were cooled down to the low temperature of the experiment, and their time-of-flight (TOF) spectra recorded up to an integrated proton current (IPC) of 344.1 and 3451.4 μA h for the aluminium and the quartz container, respectively. Then the hydride samples were placed in the cryostat at $T = 20$ K for the IINS measurements. The raw neutron scattering spectra of AlkH exhibited a series of strong features (in the 50–125 meV range, as shown in figure 1) related to the optical part of the DoPS, and mainly due to the H^- and Alk^+ anti-phase motion in the lattice unit cell. The first overtones of optical bands are also clearly visible in the recorded spectra at about twice the aforementioned energy transfer intervals. In contrast, at low energy transfer, the acoustic bands appear weaker than the optical one, since here metal and hydrogen ions move basically in phase, and the H mean square displacement is much smaller. It is worth noting the remarkable similarity of the spectra of three heaviest AlkH (i.e. KH, RbH and CsH), as well as the shift of the peaks towards lower energies while increasing the atomic number of the metal in the sample. The NaH spectrum, however, shows qualitatively different features (for example the clear emergence of the peak at about 110 meV and the almost reversed intensity ratio of the doublet in the region 150–200 meV). In this respect we might consider NaH as a sort of intermediate compound in the alkali metal hydrides series, exhibiting a behaviour between those of LiH (see [8]) and the three heaviest AlkH, which is usually observed in crystal chemistry.

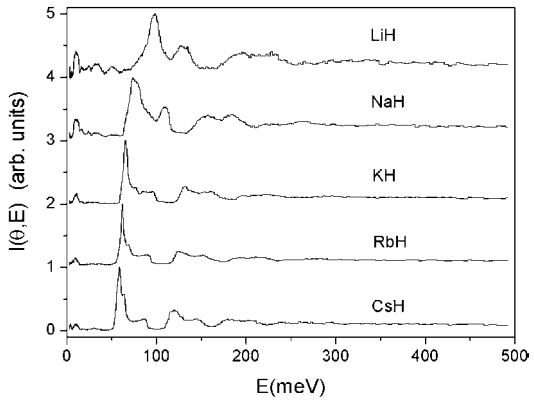

Figure 1. Raw neutron spectra of the various alkali metal hydrides measured on TOSCA-II at $T = 20$ K. LiH [8, 9] is also included for completeness of the series. The spectra have been normalized to the same peak height.

3. Data analysis

The experimental back-scattering TOF spectra were transformed into energy transfer data, detector by detector, making use of the standard TOSCA-II routines available on the spectrometer. The spectra were added together into a single data block (disregarding the forward-scattering data because of their larger instrumental background). This grouping procedure was justified by the narrow angular range spanned by the detectors, since the corresponding full width at half-maximum, $\Delta\theta$, was estimated to be only 8.32° [13]. In this way, we produced double-differential cross-section measurements along the TOSCA-II kinematic path $(Q(E), E)$ of the (AlkH sample + can) systems, plus, of course, the empty cans. Data were then corrected for the k_1/k_0 kinematic factor [14], and the empty-can contributions were properly subtracted. At this stage the important corrections for *self-absorption* attenuation and *multiple-scattering* contamination were performed, the former being particularly important for Cs hydride ($\sigma_{\mathrm{abs}}(\mathrm{Cs}) = 29.0$ b (barns) [14]). These two corrections were applied to the experimental data through the analytical approach suggested by Agrawal in the case of a flat slab-like sample [15].

As explained in section 4, we also produced *ab initio* lattice dynamics simulations, which provided us with H-projected and Alk-projected DoPS. The former, $Z_{\mathrm{H}}(E)$, reads

$$Z_{\mathrm{H}}(E) = \frac{1}{3N} \sum_{\mathbf{q}} \sum_{j=1}^{6} |\boldsymbol{\sigma}_{\mathrm{H}}(\mathbf{q}, j)|^2 \, \delta(E - E(\mathbf{q}, j)), \tag{1}$$

where $\mathbf{q}$ is a phonon wavevector contained in the first Brillouin zone, N is the number of these wavevectors, j labels the six phonon branches, $\boldsymbol{\sigma}_{\mathrm{H}}(\mathbf{q}, j)$ is a polarization vector for H and $E(\mathbf{q}, j)$ is the phonon energy. The existence of six phonon branches (three acoustic and three optical) in these compounds is caused by their rock-salt structure, implying the presence of two atoms per asymmetric unit cell: H and the alkali metal. Simulated DoPS were important for the evaluation of:

(1) The H total scattering cross-section, known to be largely dependent on E_0.
(2) An estimate of AlkH scattering law to be folded, with itself, in order to generate the multiple-scattering contributions.

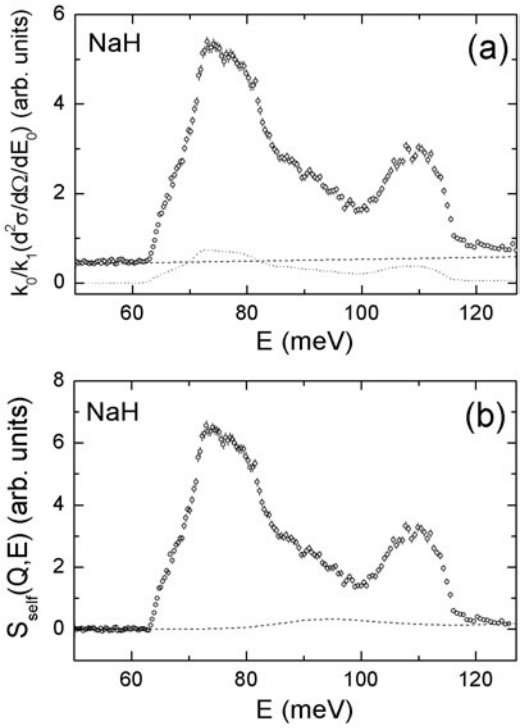

Figure 2. Evaluation of the double-inelastic-scattering (dotted curve in panel (a)) and multiphonon contributions (dashed curve in panel (b)) for NaH at $T = 20$ K, together with the TOSCA-II experimental data (empty circles with error bars in both panels). In panel (a) the estimate of the sample-dependent background has also been reported (dashed line).

Both procedures (i.e. self-absorption and multiple-scattering corrections) were accomplished in the framework of the incoherent approximation [14]. This is totally justified by the preponderance of scattering from the H ions and by the polycrystalline nature of the samples.

The main multiple-scattering term was the one including one elastic event plus one inelastic event ('*1 el. + 1 inel.*'). After a careful analysis it was also found that '*1 el. + 1 inel.*' was practically identical to the single-inelastic-scattering term ('*1 inel.*'). For this reason it was decided to limit the multiple-scattering subtraction procedure to the removal of the double inelastic events, '*2 inel.*' (further multiple-scattering contributions were found to be insignificant). Double-inelastic-scattering contributions were found modest, but not completely negligible, in the energy transfer range of interest (i.e. the optical phonon branch: 50 meV $< E <$ 125 meV), and were subtracted (see figure 2). After performing the two aforementioned corrections, our neutron spectra still contained some scattering from the alkali ions, which was however much lower than that from the H, and, moreover, mainly localized in the acoustic phonon region [10, 16], i.e. for $E < 30$ meV. This hypothesis was confirmed by the calculation of the alkali contributions to the scattering (made through the mentioned *ab initio* simulations and always in the framework of the incoherent approximation). Such a contribution turned out to be totally negligible in the optical phonon region. The other practical details concerning these procedures can be found in [8] and [17], where they were applied to various binary solid systems, such as LiH, and H_2S, D_2S, HCl, respectively. After subtracting the multiple scattering, a modest and rather flat sample-dependent background was

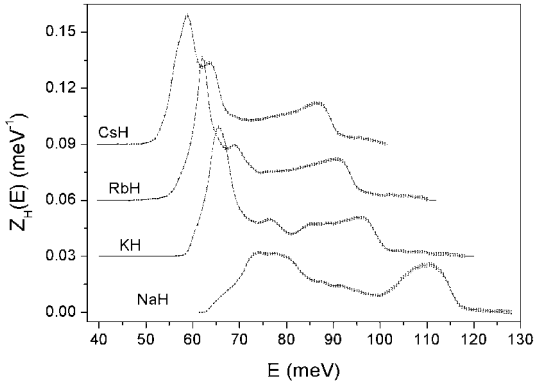

Figure 3. Optical branches of the hydrogen-projected density of phonon states at $T = 20$ K, extracted from the inelastic neutron scattering spectra (curves with error bars). From bottom to top: NaH, KH, RbH and CsH.

also estimated through a linear function of energy and removed from the processed experimental data.

The last procedure before the extraction of the H-DoPS was the evaluation and the subtraction of the multiphonon contributions, containing both optical-plus-acoustic combinations and optical-plus-optical overtones. They were not completely negligible because of the relatively high Q-values attained by TOSCA-II in the 3 meV $< E <$ 125 meV experimental range, namely 2.8 Å^{-1} $< Q <$ 8.8 Å^{-1} (in back-scattering). At this stage, the processed AlkH data were proportional to the *self*-inelastic structure factor [14] for the H ions, $S_{\rm self}(Q, E)$. Due to the isotropic nature of the crystals (which are all face-centred cubic), such a quantity can be easily interpreted as the sum of spherically averaged n-phonon terms ($n = 0, 1, 2\ldots$), each describing a neutron scattering process of creation or annihilation of n vibrational quanta in the crystal lattice. As far as the H-DoPS is concerned, the only useful contribution of the experimental spectrum is the one-phonon component of $S_{\rm self}(Q, E)$, namely $S_{\rm self,+1}(Q, E)$. The following equation shows its relation with the H-projected density of phonon states:

$$S_{\rm self,+1}(Q, E) = \frac{\hbar^2 Q^2}{4M_{\rm H}} \exp\left[-2W_{\rm H}(Q)\right] \frac{Z_{\rm H}(E)}{E} \left[\coth\left(\frac{E}{2\,k_{\rm B}T}\right) + 1\right], \qquad (2)$$

where $M_{\rm H}$ is the proton mass, $k_{\rm B}$ is the Boltzmann constant and $2W_{\rm H}(Q)$ is the well-known Debye–Waller factor, related to the mean square displacement of H (and to the H-DoPS itself) via

$$2W_{\rm H}(Q) = \frac{1}{3} Q^2 \left\langle \mathbf{u}_{\rm H}^2 \right\rangle = \frac{\hbar^2 Q^2}{2M_{\rm H}} \int_0^\infty \frac{Z_{\rm H}(\varepsilon)}{\varepsilon} \coth\left(\frac{\varepsilon}{2\,k_{\rm B}T}\right) {\rm d}\varepsilon. \qquad (3)$$

The full expansion of $S_{\rm self}(Q, E)$ in terms of phonon operators (e.g. see [18]) was employed in combination with the simulated H-projected DoPS to evaluate the multiphonon scattering. Its contribution in the optical-band energy range (50–125 meV) is low but not completely negligible, at least for NaH, as shown in figure 2. Thus experimental $S_{\rm self}(Q, E)$ spectra were analysed through an iterative procedure [19], aiming to simultaneously extract $Z_{\rm H}(E)$ and $2W_{\rm H}(Q)$, by means of (2) and (3). The technicalities can be found in [8] and [17], while the experimental $Z_{\rm H}(E)$ determinations obtained are reported in figure 3. Finally, a test on the H-DoPS extraction was performed through the A-CLIMAX code [20], which, starting from $Z_{\rm H}(E)$, can simulate the $S_{\rm self}(Q, E)$ spectrum measured by TOSCA-II. The agreement

Table 2. Mean square displacements $\langle \mathbf{u}_H^2 \rangle$, mean kinetic energies $\langle T_H \rangle$ and Einstein frequencies $\Omega_{0,H}$ of hydrogen in alkali hydrides at $T = 20$ K from the present inelastic neutron scattering measurements. Energy shifts δE used to optimize the agreement between experimental and simulated ABINIT data are also reported.

Sample	$\langle \mathbf{u}_H^2 \rangle$ (Å^2)	$\langle T_H \rangle$ (meV)	$\hbar\Omega_{0,H}$ (meV)	δE (meV)
NaH	0.0736(4)	66.9(4)	90.7(5)	−13.25
KH	0.0856(5)	57.7(4)	78.2(6)	4.30
RbH	0.0893(4)	55.0(2)	74.4(4)	5.10
CsH	0.0953(3)	51.3(2)	69.5(3)	7.40

found between experimental and A-CLIMAX spectral results was totally satisfactory for all the present samples.

From these $Z_H(E)$ data, making use of normal and Bose-corrected moment sum rules [18], we were also able to derive three important physical quantities related to hydrogen dynamics in these hydrides, namely: the H *mean square displacement* $\langle \mathbf{u}_H^2 \rangle$, the H *mean kinetic energy* $\langle T_H \rangle$ and the H *Einstein frequency* $\Omega_{0,H}$, all reported in table 2.

4. Lattice dynamics simulations

The vibrational dynamics of the heavy AlkH lattices has been simulated by the present authors through two entirely different approaches, namely: (i) a totally *ab initio* method based on the density functional theory and making use of pseudopotentials and a plane-wave basis, and (ii) a more standard lattice dynamics employing *semi-empirical inter-atomic potentials*.

As for the first approach, calculations were carried out using the plane-wave density functional theory as implemented in the ABINIT code [21]. Here, two main limitations occur. The first is the use of pseudopotentials to represent the core electrons, allowing us only to include relativistic effects in an essentially non-relativistic code. This choice is of the maximum importance for reducing the number of plane waves representing the electronic wavefunction to a level that is tractable with the currently available computer power. The second limitation concerns the use of the density functional theory, where two general approaches apply: in the local density approximation (LDA) the exchange and correlation energies are described as functions of the local electron density at each point, while in the generalized gradient approximation (GGA), electron density gradients are also taken into account. It has been shown that the GGA provides results in better agreement with experimental data than those obtained from the LDA when low-Z elements are involved. However, the opposite is found if high-Z elements are considered. On the other hand, Bellaiche *et al* [22] have calculated the equation of state for LiH and LiD using Hartree–Fock theory and two different LDA functionals, considering both the pseudopotential and the all-electron approaches. Results from Hartree–Fock and LDA approaches differ less than 1%, indicating that, at least for this system, the equation of state depends only very weakly on the electron correlation. Because, in principle, for the solid state, neither LDA nor GGA have clearly proved their superiority, it was decided to carry out all the AlkH simulations considering the LDA (less demanding as regards computer time), using the Teter–Padé parametrization [23] and the norm-conserving Troullier–Martins pseudopotentials [24]. The only exception was represented by the potassium ion in KH, where the Hartwigsen–Goedecker–Hutter pseudopotential had to be employed [25]. It was carefully verified for all simulations that full convergence was achieved as regards both the number of k-points in the reciprocal space and the energy cut-off of the plane waves. So, the final choice in the AlkH calculations was a mesh of $8 \times 8 \times 8$ points in the reciprocal space

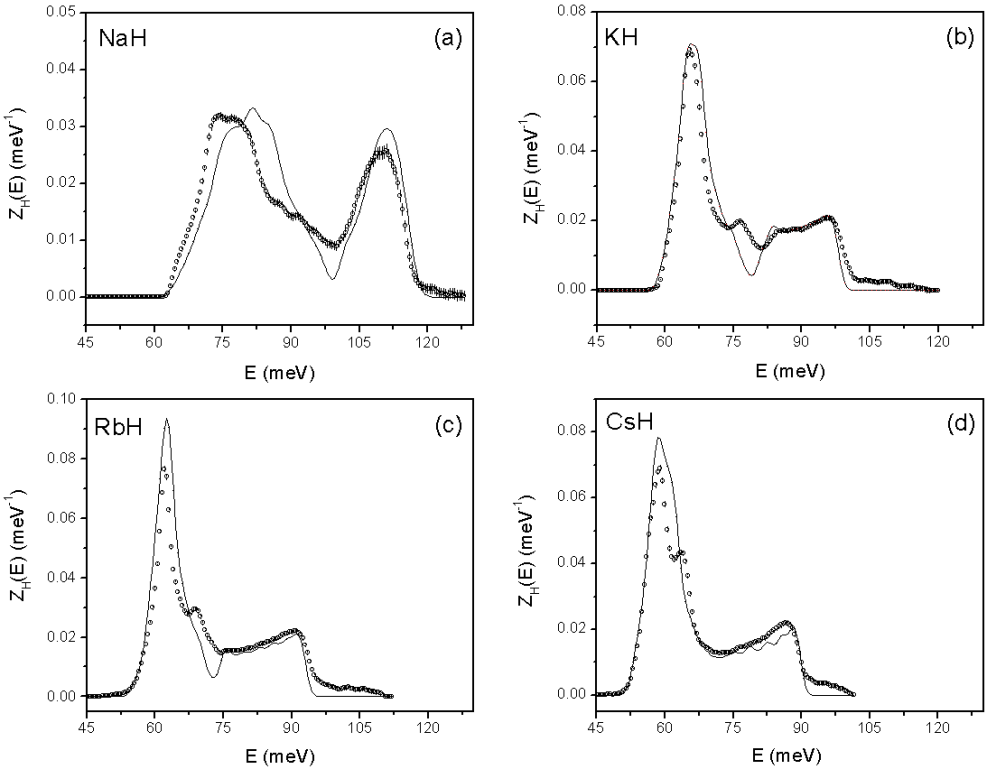

Figure 4. Comparison between experimental and simulated optical branches of the hydrogen-projected density of phonon states: neutron scattering experimental results (empty circles with error bars) and ABINIT simulations (full curve). The panels from (a) to (d) show NaH, KH, RbH and CsH, respectively.

(This figure is in colour only in the electronic version)

and a cut-off of 1360 eV. ABINIT results for $Z_{\mathrm{H}}(E)$ and dispersion curves, $\omega_j(\mathbf{q})$, are plotted in figures 4 and 5, respectively.

Additional lattice dynamics simulations have been performed making use of semi-empirical inter-atomic pair potentials (HS) proposed by Hussain and Sangster [12]. This approach was meant to include alkali hydrides in a larger potential scheme devised by Sangster *et al* [26], and derived for the complete set of alkali halides. HS includes four inter-atomic pairwise contributions: the long-range Coulomb interaction; the Born–Mayer functional form describing the short-range inter-ionic repulsion; and two weak short-range terms accounting for the dipole–dipole and the dipole–quadrupole van der Waals attractions. As for the short-range terms between the atomic species α and β, $V_{\mathrm{SR}}^{(\alpha,\beta)}(r)$, one writes

$$V_{\mathrm{SR}}^{(\alpha,\beta)}(r) = \beta_{\alpha,\beta}\exp(-\alpha_{\alpha,\beta}r) - \frac{C_{\alpha,\beta}}{r^6} - \frac{D_{\alpha,\beta}}{r^8}, \tag{4}$$

where the twelve HS parameters are taken from [12] and [26]. As regards the long-range Coulomb terms, a common value of the ionic charge was assumed ($Z = 0.97$) for all the AlkH, following [26], and simple harmonic shell–core models were implemented to describe the various ionic polarizabilities. The HS inter-atomic potentials have been plugged into the general utility lattice program GULP [27], which, after performing the lattice energy

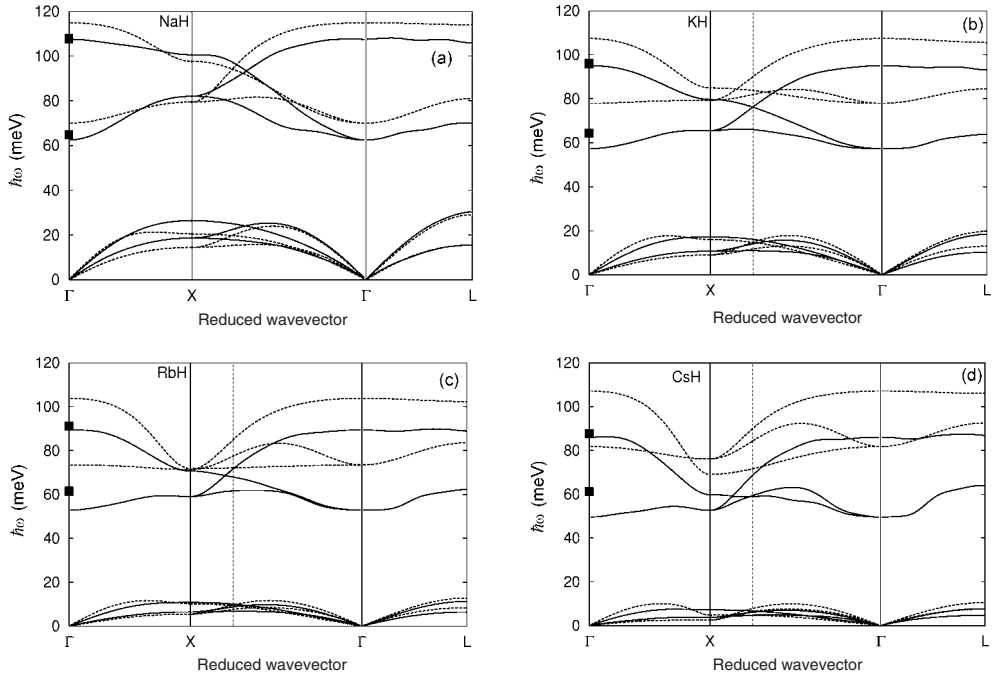

Figure 5. Acoustic and optical branches of phonon dispersion curves, including ABINIT simulations (full curves) and SM lattice dynamics results [10] (dashed curves). The panels from (a) to (d) show NaH, KH, RbH and CsH, respectively. Full squares on the left side represent the Γ-point energy values of the transverse and longitudinal optical branches simulated by Zinenko and Fedorov [3].

minimization (results for lattice parameters and cohesive energies are reported in table 1 of [12]), evaluated $Z_{\mathrm{H}}(E)$ for the heavy alkali hydrides (see figure 6). It is worth noting that CsH is not included since the HS potential scheme seems to fail even in the description of its static properties.

5. Discussion

Our experimental determinations of the H-projected densities of phonon states in heavy alkali metal hydrides (see figure 3) contain detailed information on the hydrogen self-dynamics in such compounds, especially as regards its dependence on the cation atomic number Z and on the lattice constant a_{exp}. As we have already mentioned in section 1, there is no previous experimental study available on $Z_{\mathrm{H}}(E)$ in these systems (except a preliminary report about NaH [9]); thus the present work fills a large gap in the understanding of the H vibrational dynamics in ionic hydrides. In figure 4 a detailed comparison between IINS and ABINIT H-DoPS curves is shown: one observes a satisfactorily good agreement in the case of KH, RbH and CsH. As for NaH, the comparison between experiment and simulation is globally acceptable, but not so good as for the other hydrides. For example, the position of the first $Z_{\mathrm{H}}(E)$ peak (due to the transverse optical phonon band) is not precisely reproduced by ABINIT. A clearly remarkable feature is represented by the strong similarity of the H-projected densities of phonon states of the last three AlkH: it suggests that KH, RbH and CsH could be gathered together in a sub-group of compounds rather different from LiH [9, 16], NaH being a sort of 'crossover' alkali metal hydride. It is worth noting that the simulated H-DoPS

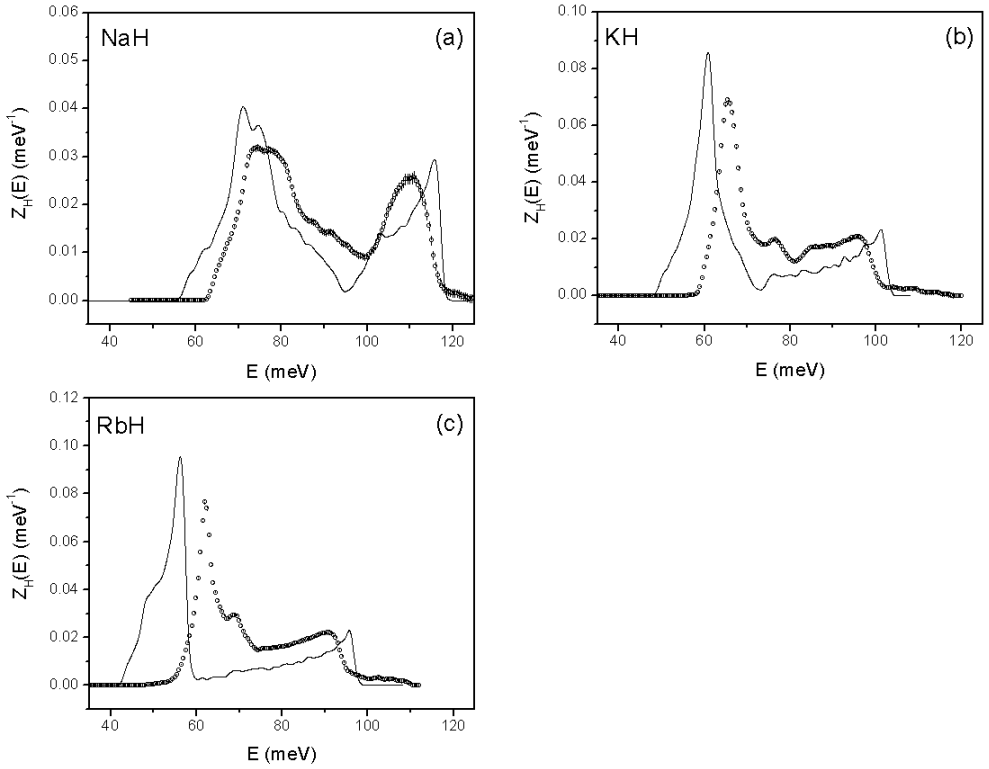

Figure 6. Comparison between experimental and simulated optical branches of the hydrogen-projected density of phonon states: neutron scattering experimental results (empty circles with error bars) and GULP simulations (full curve). The panels from (a) to (c) show NaH, KH and RbH, respectively.

curves in figure 4 have been slightly shifted (rigidly) in order to optimize their agreement with the experimental $Z_H(E)$ (see also table 2). This procedure (or alternatively the use of a scaling factor) is not at all uncommon in dealing with *ab initio* vibrational energies [28], and it does not alter the overall spectral shape of the H-DoPS. In addition, the effect of the experimental energy resolution has been checked and found irrelevant in the present spectral range (50 meV $< E <$ 125 meV). Together with the phonon energy calculations, ABINIT code has also provided reliable estimates of AlkH lattice constants (see [29]), whose discrepancies from the experimental values [30] are always lower than 1%.

The aforementioned scenario cannot be exactly applied to the results derived from the atomistic simulations using the GULP code too, at least when dealing with the H-DoPS. First of all, the HS potential scheme is totally unable to describe CsH [12], even though the static lattice properties (i.e. a_{hs}, U_{hs}) of the remaining heavy AlkH come out reasonably close to their experimental values (the discrepancies being always lower than 2%, for both cohesive energies and lattice constants). However, as far as the $Z_H(E)$ simulations obtained from HS are concerned (see figure 6), it is evident that the agreement with the present experimental data is only qualitative, and clearly degrading as Z increases. For this reason no energy shift (or energy scaling) was even attempted to match GULP results and IINS data.

The limitations of the HS potentials for describing the H vibrational dynamics in AlkH are not totally surprising: even the simulated LiD dispersion curves [12] did not turn out to

be in perfect agreement with the measured neutron data [7]. This is particularly significant since some of the LiH static and dynamic properties were actually employed to work out six general parameters of the HS potential scheme [12], so a good description of the LiH/LiD lattice dynamics would have been expected. One physical reason for the aforementioned HS limitations is probably the simplicity of the shell model proposed (which includes only pair potential terms), not completely accounting for the complexity of the hydrogen–cation interactions [29]. However, as already pointed out by Haque and Islam [4], the main criticism of HS is the ambition to describe all alkali metal halides plus AlkH in the same potential scheme: as shown by the Haque and Islam, independent Born–Mayer pair potentials for LiH and NaH can provide a better description of some physical properties of these two systems.

The last point to be discussed concerns the SM, the force constant model proposed by Dick and Jex [10] and briefly described in section 1. We evaluated the various SM phonon dispersion curves for the heavy AlkH, and we have plotted them in figure 5 together with ABINIT ones (already energy shifted as in table 2). The first feature to be noted is the degeneracy of the two transverse optical branches in the direction [1, 0, 0] from Γ to X, and in the direction [1, 1, 1] from Γ to L. One can say that it is an aspect of a more general property of transverse modes in high-symmetry situations: where there are threefold, fourfold or sixfold rotation axes along the direction of the reduced wavevector, the force constants will be the same for any two transverse displacements, so the two transverse modes will have degenerate frequency dispersion. This is exactly the case in the directions [1, 0, 0] and [1, 1, 1]. Another interesting characteristic of the ABINIT data is the lowering of both transverse and longitudinal optical branches while the cation atomic number increases. This fact was also evident from the H-DoPS in figure 4, but it is now made even clearer. In addition, one can observe the behaviour of the transverse optical branches, which become globally flatter moving from NaH to CsH; however, some dispersion is still present and clearly visible. This can be interpreted as the effect of a residual long-range interaction between H ions. In the SM calculations of the dispersion curves for CsH (see figure 5, panel (d); and for CsD, as in [10]), the high polarizability of the cations seems to force the longitudinal optical mode below the transverse optical one in the [1, 0, 0] direction, close to the symmetry point X. However, the ABINIT results appear to contradict this peculiar finding, which, on the other hand, was considered very unlikely even by Dyck and Jex themselves [10]. This difference has to be ascribed to a better description of the interaction between second-nearest neighbours in ABINIT as compared to the SM.

The SM calculations are in fairly good agreement with ABINIT ones only in the case of NaH, so the limitations of this force constant model in the case of the KH/RbH/CsH sub-group are probably due to the assumptions implicit in the Dyck and Jex approach itself: the force constants were estimated using LiD phonon data only, and then a complex scaling mechanism was hypothesized to build the SM force constant scheme for the heavy alkali metal hydrides. Despite the ingenuity of this idea, the scaling seems to work reasonably well for Na only, tending to worsen as the cation atomic number, Z, grows. At this stage, it is worth noting that final conclusions on the phonon dispersion curves in AlkH could be drawn only from coherent inelastic neutron (or x-ray) scattering experiments. However, the actual measurements on large single crystals of NaH, KH, RbH and CsH (or better, on their deuterated versions) seem rather improbable at the moment, since these compounds are highly unstable and completely dissociated before melting. Only LiH/LiD can be easily liquefied and crystallized, and this is the main reason that an experimental determination of its dispersion curves is available [7]. Thus the use of incoherent inelastic neutron scattering was almost mandatory in our case, even though we are well aware that our approach (i.e. matching IINS and ABINIT H-DoPS through an energy shift of the latter, and then applying the same shift to the ABINIT dispersion curves) was not rigorous, since it is well known that $Z_{\mathrm{H}}(E)$ and optical dispersion curves are not linked

by a one-to-one relation [18]. However, we are totally convinced that an important assessment of the quality and the limitations of the SM model can be obtained in this way. Finally, an independent check on the energy-shifted ABINIT dispersion curves is provided by the Γ-point energy values of the transverse and longitudinal optical branches simulated by Zinenko and Fedorov [3] and reported in figure 5. Although their agreement with the ABINIT dispersion curves at the Γ point is not always perfect, it is good enough to indicate the inadequacy of the SM ones for the KH/RbH/CsH group.

6. Conclusion and perspective

In the present paper we have reported incoherent inelastic neutron scattering spectra from alkali metal hydrides (NaH, KH, RbH and CsH), measured at $T = 20$ K in the energy and momentum transfer ranges 3 meV $< E <$ 500 meV and 2.8 Å^{-1} $< Q <$ 16.5 Å^{-1}. From the medium-energy region of these spectra (namely 50–125 meV, coinciding with the optical phonon bands), we were able to extract accurate hydrogen-projected densities of phonon states. These experimental phonon distributions were then compared to the equivalent results obtained from *ab initio* lattice dynamics simulations, operated through the ABINIT code [21], and based on density functional theory and pseudopotentials. The overall agreement between neutron and *ab initio* data turned out to be very good—especially impressive for the three heaviest compounds (KH, RbH and CsH). This finding proves that, at least for this simple class of binary compounds, a quantitative agreement between experimental and *ab initio* data is possible, not only for static (lattice parameters) and macroscopic quantities (bulk modulus, cohesive energy etc), but also for the issue of the microscopic hydrogen dynamics. Phonon dispersion curves were also derived from the *ab initio* simulations. After a general discussion, these curves were compared to the results of a shell-model lattice dynamics calculation [10], in which the main parameters were extrapolated from coherent neutron scattering data on LiD [7].

Further lattice dynamics calculations, based on a pairwise Born–Mayer semi-empirical potential scheme [12, 26], were also performed, providing only an approximate and qualitative agreement with the experimental neutron data and quickly degrading as the cation atomic number increases. Thus the incoherent inelastic neutron spectroscopy technique has proved to be not only a reliable method for the investigation of the H dynamics in metal hydrides [31], but also a stringent and demanding validation tool for application to the lattice dynamics simulations of these technologically relevant materials. These conclusions pave the way for a broader investigation of more complex compounds such as alkaline-earth hydrides, borohydrides and aluminohydrides.

Acknowledgments

The skilful technical help of the ISIS User Support Group is gratefully acknowledged. *Ab initio* results have been obtained through the use of the ABINIT code, a common project of the Université Catholique de Louvain (Belgium) and other contributors (URL: www.abinit.org). In addition, Dr J D Gale, (Imperial College, London, UK) is warmly thanked for kindly providing us with his GULP code. GDB thanks Consejo Nacional de Investigaciones Científicas y Técnicas (CONICET) for partial financial support. AJRC and GDB thank the Centre for Molecular Structure and Dynamics (CMSD) for financial assistance for GDB's visit.

References

[1] Mueller W M, Blackledge J P and Libowitz G G 1968 *Metal Hydrides* (New York: Academic)
[2] Zintl E and Harder A 1931 *Z. Phys. Chem.* B **14** 265

[3] Zinenko V I and Fedorov A S 1994 *Sov. Phys.—Solid State* **36** 742
[4] Haque E and Islam A K M A 1990 *Phys. Status Solidi* b **158** 457
Islam A K M A 1993 *Phys. Status Solidi* b **180** 9
[5] Besson J M, Weill G, Hamel G, Nelmes R J, Loveday J S and Hull S 1992 *Phys. Rev.* B **45** 2613 and references therein
[6] Ho A C, Hanson R C and Chizmeshya A 1997 *Phys. Rev.* B **55** 14818 and references therein
[7] Verble J L, Warren J L and Yarnell J L 1968 *Phys. Rev.* **168** 980
[8] Boronat J, Cazorla C, Colognesi D and Zoppi M 2004 *Phys. Rev.* B **69** 174302
[9] Woods A D B, Brockhouse B N, Sakamoto M and Sinclair R N 1961 *Inelastic Scattering of Neutrons in Liquids and Solids* (Vienna: IAEA) p 487 (contains raw neutron spectra from LiH and NaH)
Colognesi D, Ramirez-Cuesta A J, Zoppi M, Senesi R and Abdul-Redah T 2004 *Physica* B at press (contains a preliminary account on LiH and NaH densities of phonon states)
[10] Dyck W and Jex H 1981 *J. Phys. C: Solid State Phys.* **14** 4193
[11] Ruoff A L, Ghandehari K, Luo H, Trail S S, Di Salvo F J and Bucher G L 1996 *Solid State Commun.* **100** 777
[12] Hussain A R Q and Sangster M J L 1986 *J. Phys. C: Solid State Phys.* **19** 3535
[13] Colognesi D, Celli M, Cilloco F, Newport R J, Parker S F, Rossi-Albertini V, Sacchetti F, Tomkinson J and Zoppi M 2002 *Appl. Phys.* A **74** 64
[14] Lovesey S W 1987 *Theory of Neutron Scattering from Condensed Matter* vol 1 (Oxford: Oxford University Press)
[15] Agrawal A K 1971 *Phys. Rev.* A **4** 1560
[16] Zemlianov M G, Brovman E G, Chernoplekov N A and Shitikov Yu L 1965 *Inelastic Scattering of Neutrons* vol 2 (Vienna: IAEA) p 431
[17] Colognesi D, Andreani C and Degiorgi E 2003 *J. Neutron Res.* **11** 123
[18] Turchin V F 1965 *Slow Neutrons* (Jerusalem: Israel Program for Scientific Translations)
[19] Kolesnikov A I and Li J-C 1997 *Physica* B **234–236** 34
Dawidowski J, Bermejo F J and Granada J R 1998 *Phys. Rev.* B **58** 706
[20] Ramirez-Cuesta A J 2004 *Comput. Phys. Commun.* **157** 226
[21] Gonze X, Beuken J-M, Caracas R, Detraux F, Fuchs M, Rignanese G-M, Sindic L, Verstraete M, Zerah G, Jollet F, Torrent M, Roy A, Mikami M, Ghosez Ph, Raty J-Y and Allan D C 2002 *Comput. Mater. Sci.* **25** 478
[22] Bellaiche L, Besson J M, Kunc K and Lévy B 1998 *Phys. Rev. Lett.* **80** 5576
[23] Goedecker S, Teter M and Hutter J 1996 *Phys. Rev.* B **54** 1703
Perdew J P, Burke K and Ernzerhof M 1996 *Phys. Rev. Lett.* **77** 3865
[24] Troullier N and Martins J L 1991 *Phys. Rev.* B **43** 1993
[25] Hartwigsen C, Goedecker S and Hutter J 1998 *Phys. Rev.* B **58** 3641
[26] Sangster M J L, Schröder U and Atwood R M 1978 *J. Phys. C: Solid State Phys.* **11** 1523
[27] Gale J D 1996 *Phil. Mag.* B **73** 3
Gale J D 1997 *J. Chem. Soc. Faraday Trans.* **93** 629
[28] Foresman J B and Frisch A 1993 *Exploring Chemistry with Electronic Structure Methods* 2nd edn (Pittsburgh, PA: Gaussian)
[29] Barrera G D, Colognesi D, Mitchell P C H, Ramirez-Cuesta A J and Zoppi M 2004 in progress
[30] Wyckoff R W G 1963 *Crystal Structures* vol 1 (New York: Interscience)
[31] Ross D K 1997 *Hydrogen in Metals* vol 3, ed H Wipf (Berlin: Springer) p 153